Inorg. Chem. **2009**, *48*, 1542−1550

Nanostructured ZnS and CdS Films Synthesized using Layered Double Hydroxide Films as Precursor and Template

Birgit Schwenzer,[†] Lia Z. Pop,[‡] James R. Neilson,[†,‡,§] Timothy B. Sbardellati,[‡] and Daniel E. Morse*[,†,‡,§]

Institute for Collaborative Biotechnologies, California NanoSystems Institute, and the Materials Research Laboratory, University of California, Santa Barbara, California 93106

Received September 30, 2008

Anion exchange reactions in layered double hydroxide films ($M(OH)_{2-x}(NO_3)_x \cdot mH_2O$) followed by solid state conversion reactions are shown to yield micrometer-sized unsupported metal sulfide (M = Zn, Cd) films with unique textured morphologies. The characteristic three-dimensional nanostructured film morphology and crystallinity of the initial films are retained in the metal sulfide films although these conversion reactions involve anion exchanges concomitant with significant rearrangements of the crystal structures. Surface areas of 42 m^2/g for zinc sulfide and 50 m^2/g for cadmium sulfide thin films are observed. These values correspond to an increase in surface area of 75% for the $Zn_5(OH)_8(NO_3)_2 \cdot 2H_2O$ to zinc sulfide conversion, while the cadmium sulfide films exhibit more than three times the surface area of their precursor material, $Cd(OH)(NO_3) \cdot H_2O$. The three-dimensional morphology of the resulting films is thus observed to combine the physical properties of the bulk materials with the advantages of higher surface areas typically associated with nanostructured or porous materials. The layered double hydroxide materials used in this study to provide both structural and chemical templates were prepared using the mild conditions of a biologically inspired vapor-diffusion catalytic synthesis.

Introduction

Solid state conversion reactions in which the shape and size of the starting material are retained are frequently employed to prepare related materials in morphologies that cannot readily be synthesized otherwise. Because solid state conversion reactions depend on the diffusion of one reagent into the crystal lattice of another, reports of successful solid state conversion reactions at low temperatures are mostly limited to nanometer-sized structures.[1] Metal oxide,[2] metal chalcogenide,[3] metal nitride,[4] and intermetallic[5] nanoparticles and nanowires have been prepared using this approach. The synthesis of nanostructures by wet-chemical or by solid state reactions often relies on the use of spatial confinement in the form of nanoscale reaction vessels (nanoreactors) to control particle size and shape. Depending on the synthesis conditions for the formation of the desired nanostructures, protein cages,[6] micelles,[7] zeolites,[8] and anodically etched alumina membranes[9] all have been used to shape nanomaterials in situ. A few studies also report the use of layered double hydroxide structures as host materials for nanoparticle synthesis.[10]

Layered double hydroxides (LDHs) constitute a class of inorganic hydroxide materials that consist of positively

* To whom correspondence should be addressed. E-mail: d_morse@lifesci.ucsb.edu. Fax: +001-805-893-7998. Phone: +001-805-893-7442.
† Institute for Collaborative Biotechnologies, California NanoSystems Institute, and the Materials Research Laboratory.
‡ Department of Molecular, Cellular and Developmental Biology, University of California, Santa Barbara, California 93106.
§ Biomolecular Science and Engineering Graduate Program, University of California, Santa Barbara, California 93106.

(1) Vasquez, Y.; Henkes, A. E.; Bauer, J. C.; Schaak, R. E. *J. Solid State Chem.* **2008**, *181*, 1509.
(2) Shevchenko, E.; Kortright, J. B.; Talapin, D. V.; Shaul, A.; Alivisatos, A. P. *Adv. Mater.* **2007**, *19*, 4183.
(3) (a) Zhang, H.; Yang, D.; Ma, X.; Que, D. *Nanotechnology* **2005**, *16*, 2721. (b) Yan, C.; Xue, D. *J. Phys. Chem. B* **2006**, *110*, 25850.
(4) (a) Gao, L.; Zhang, Q.; Li, J. *J. Mater. Chem.* **2003**, *13*, 154. (b) Schwenzer, B.; Loeffler, L.; Seshadri, R.; Keller, S.; Lange, F. F.; DenBaars, S. P.; Mishra, U. K. *J. Mater. Chem.* **2004**, *14*, 637.
(5) Vasquez, Y.; Zhiping, L.; Schaak, R. E. *J. Am. Chem. Soc.* **2008**, *130*, 11866.
(6) Wong, K. K. W.; Mann, S. *Adv. Mater.* **1996**, *8*, 928.
(7) Koh, H.-D.; Kang, N.-G.; Lee, J.-S. *Langmuir* **2007**, *23*, 11425.
(8) Sathish, M.; Viswanathan, B.; Viswanath, R. P. *Int. J. Hydrogen Energy* **2006**, *31*, 891.
(9) Gavrilov, S.; Nosova, L.; Sieber, I.; Belaidi, A.; Dloczik, L.; Dittrich, T. *Phys. Status Solidi A* **2005**, *202*, 1497.
(10) Lukashin, A. V.; Eliseev, A. A.; Zhuravleva, N. G.; Kalinin, S. V.; Vergetel, A. A.; Tret'yakov, Y. D. *Doklady Chem.* **2002**, *383*, 93.

10.1021/ic801865w CCC: $40.75
Published on Web 01/16/2009

charged brucite-type sheets of edge-sharing $M(OH)_6$ octahedra, counterbalanced by anions intercalated between the layers. LDHs also are referred to as hydrotalcite-like materials for their similarity to the mineral $[Mg_6Al_2(CO_3)(OH)_{16}\cdot 4H_2O]$. A wide variety of LDH structures can be found in natural minerals, while over the last 15 years many new LDH materials with the general composition $[M^{2+}_{1-x}M^{3+}_x(OH)_2]^{x+}(A^{n-})_{x/n}\cdot mH_2O$ or $[M^{1+}_{1-x}M^{4+}_x(OH)_2]^{x+}(A^{n-})_{x/n}\cdot mH_2O$ have been synthesized.[11] For a subcategory of LDHs, the so-called layered hydroxide salts,[12] the positive charge of the $[M(OH)_2]$ layers is not produced by the incorporation of trivalent metal ions. These compounds, $[M(OH)_{2-x}]^{x+}(A^{n-})_{x/n}\cdot mH_2O$, derive their positive net charge from replacement of some of the OH^- ions in the crystal lattice with different anions or water molecules. One such material is $Zn_5(OH)_8(NO_3)_2\cdot 2H_2O$,[13,14] a zinc hydroxide nitrate material used in this study. This material consists of layered sheets with octahedrally coordinated Zn^{2+} ions in the brucite layer. One fourth of the octahedra in every plane are unoccupied by Zn^{2+} ions, being replaced instead by two tetrahedrally coordinated Zn^{2+} ions located above and below the plane of the octahedrally coordinated Zn^{2+} ions. The crystal lattice thus exhibits a ratio of 3:2 octahedral to tetrahedral Zn^{2+} sites, resulting in an overall structure of charged cationic layers that are held together by NO_3^- counterions and intercalated water molecules.

Because of their cationic nature and inherent stability, as well as their porosity and high surface areas, LDHs are increasingly studied and used industrially as high surface area catalysts,[15] absorbants,[16] molecular sieves,[17] and in medical applications, such as time-release drug delivery agents.[18] Additionally, LDHs have been recognized as suitable for nanostructural templating.[10]

We recently reported a biologically inspired vapor-diffusion catalytic synthesis that provides a generic pathway for preparing three-dimensionally structured LDH films at room temperature in aqueous solution.[14,19] The resulting LDH films are composed of highly aligned nanoparticles (15−45 nm, depending on the material). While the synthesis method we employ starts with aqueous metal salt solutions, and is therefore similar to chemical bath deposition (CBD),[20] the kinetically controlled vapor-diffusion catalysis method yields highly structured unsupported films. In contrast, in conventional CBD the heterogeneous nucleation on substrates produces untextured thin films.[20] Details of this environmentally friendly, low-temperature and low-cost synthesis method for metal hydroxide, phosphate, and oxide films have been described previously.[14,19,21]

We report here the synthesis of extended three-dimensionally structured zinc sulfide (ZnS) and cadmium sulfide (CdS) films from these LDHs. To our knowledge this is the first report of micrometer-sized ZnS or CdS films with structured morphologies that have been prepared by solid state conversion reaction at temperatures below 100 °C. Instead of first intercalating a metal-containing anion into the LDH lattice for subsequent incorporation of this metal into the newly synthesized nanoparticles, as reported for example by Lukashin et al.,[10] we use the metal ions of the positively charged layers of the LDH as reagent in the solid state conversion reaction. Nanostructured LDH films of $Zn_5(OH)_8(NO_3)_2\cdot 2H_2O$[13,14] and $Cd(OH)(NO_3)\cdot H_2O$[22] provide the morphological and chemical templates for conversion to ZnS and CdS films. Thereby we have developed a low-temperature, two-step synthesis method for the preparation of uniquely textured ZnS and CdS films (50−70 μm thick) from their respective metal nitrate salts. The three-dimensional morphology of the resulting films combines the physical properties of the bulk materials, as observed in thin films, with the advantages of higher surface areas typically associated with nanostructured or porous materials.

As a first step, three-dimensionally structured films of the two LDH materials $Zn_5(OH)_8(NO_3)_2\cdot 2H_2O$[13,14] and $Cd(OH)(NO_3)\cdot H_2O$[22] are prepared using the water-based, low-temperature vapor-diffusion catalysis method.[14,19,21] In a second step the as-prepared metal hydroxide nitrate films are reacted with aqueous sodium sulfide (Na_2S). The characteristic three-dimensional nanostructured film morphology of the LDH materials, as well as the degree of crystallinity of the films, are retained in the metal sulfide films although these conversion reactions involve an anion exchange ($NO_3^- \rightarrow S^{2-}$) concomitant with significant rearrangements of the crystal structure during the OH^- to S^{2-} replacement of the solid state conversion reaction. The resulting metal sulfide films display very similar morphologies on the micrometer length scale to the original metal hydroxide nitrate films, but the overall surface areas increase significantly during the conversion reaction because of the introduction of additional mesopores into the material. Surface areas of 42 m^2/g for zinc sulfide and 50 m^2/g for cadmium sulfide thin films are observed.

Experimental Section

All starting materials used in this study were commercially available (Sigma Aldrich Co. or Alfa Aesar unless noted otherwise)

(11) Bravo-Suárez, J. J.; Páez-Mozo, E. A.; Oyama, S. T. *Quim. Nova* **2004**, *27*, 601.
(12) Arizaga, G. G. C.; Satyanarayana, K. G.; Wypych, F. *Solid State Ionics* **2007**, *178*, 1143.
(13) Stählin, W.; Oswald, H. R. *Acta Crystallogr., Sect. B* **1970**, *26*, 860.
(14) (a) Schwenzer, B.; Roth, K. M.; Gomm, J. R.; Murr, M.; Morse, D. E. *J. Mater. Chem.* **2006**, *16*, 401. (b) Schwenzer, B.; Gomm, J. R.; Morse, D. E. *Langmuir* **2006**, *22*, 9829.
(15) Tichit, D.; Gerardin, C.; Durand, R.; Coq, B. *Top. Catal.* **2006**, *39*, 89.
(16) Dadwhal, M.; Kim, T. W.; Sahimi, M.; Tsotsis, T. T. *Ind. Eng. Chem. Res.* **2008**, *47*, 6150.
(17) Zhao, H.; Vance, D. S. *Clays Clay Miner.* **1998**, *46*, 712.
(18) Xue, Y. H.; Zhang, R.; Sun, X. Y.; Wang, S. L. *J. Mater. Sci.: Mater. Med.* **2008**, *19*, 1197.
(19) Schwenzer, B.; Morse, D. E. *J. Nanomater.* **2008** Article ID 352871.
(20) (a) Ben Nasr, T.; Kamoun, N.; Kanzari, M.; Bennaceur, R. *Thin Solid Films* **2006**, *500*, 4. (b) Lincot, D.; Hodes, G. *Proc.-Electrochem. Soc.* **2006**, *2003−31*, 1. (c) Xu, X. B.; Huang, S. Y.; Cu, J. B.; Zhu, H. B.; Sun, Z.; Chen, Y. W.; Huang, S. M. *Surf. Rev. Lett.* **2008**, *15*, 265.
(21) (a) Kisailus, D.; Schwenzer, B.; Gomm, J.; Weaver, J. C.; Morse, D. E. *J. Am. Chem. Soc.* **2006**, *128*, 10276. (b) Gomm, J. R.; Schwenzer, B.; Morse, D. E. *Solid State Sci.* **2007**, *9*, 429.
(22) JCPDS file No. 00-018-0260; Technisch Physische Dienst, Delft, Netherlands.

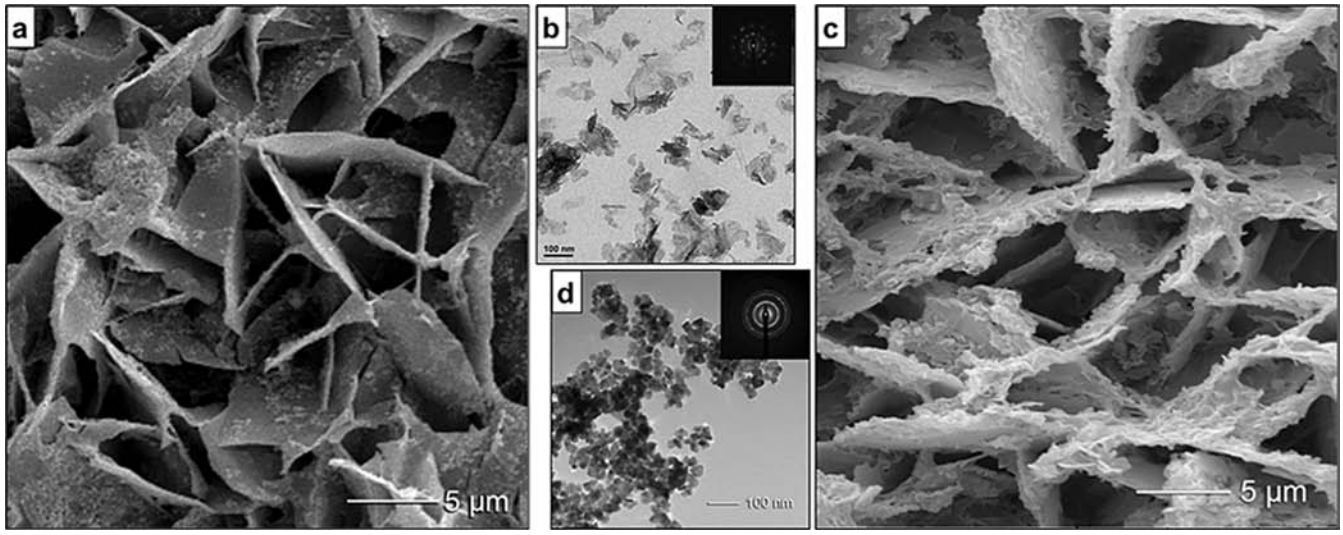

Figure 1. Nanostructured $Zn_5(OH)_8(NO_3)_2 \cdot 2H_2O$ film prepared as described in the text: (a) SEM image of the nanostructured side of the film, (b) TEM image of the ground material [inset: SAED image]; and ZnS film synthesized using as-prepared $Zn_5(OH)_8(NO_3)_2 \cdot 2H_2O$ films: (c) SEM image of the nanostructured side of the film, (d) TEM image of the ground material [inset: SAED image].

and were used without further purification. All experiments were carried out under ambient conditions in air unless noted otherwise.

Metal Hydroxide Nitrate (M = Zn, Cd) Thin Film Synthesis. $Zn_5(OH)_8(NO_3)_2 \cdot 2H_2O$[13,14] thin films were prepared by vapor-diffusion catalysis as previously described by Schwenzer et al.[14,19,21] Forty milliliters of aqueous 0.1 M $Zn(NO_3)_2 \cdot 6H_2O$ solution and 10 mL of a dilute 0.6% NH_4OH solution (EMD Chemicals, Inc.) were placed in separate, uncovered Petri dishes. The ratio of air/liquid interface areas of the two different solutions was 3:1. The containers with reaction solutions were placed together inside a sealed chamber. Within 4 h extended LDH films formed on the surfaces of the metal salt solutions.

$Cd(OH)(NO_3) \cdot H_2O$[22] thin films were prepared similarly. However, because Cd^{2+} ions exhibit greater affinity for dissolved CO_2 from the air than Zn^{2+} ions used for the formation of $Zn_5(OH)_8(NO_3)_2 \cdot 2H_2O$ as described above, this complexation of Cd^{2+} ions resulted in the preferential formation of $Cd(CO_3)_2$.[23] Therefore, the vapor-diffusion synthesis of $Cd(OH)(NO_3) \cdot H_2O$ by hydrolysis of an aqueous 0.1 M solution of $Cd(NO_3)_2 \cdot 4H_2O$ catalyzed by NH_3 (formed from NH_4OH) was carried out in a nitrogen enriched atmosphere. The reaction time was 4 h.

After formation, the unsupported films were transferred by Langmuir−Blodgett technique onto a doubly distilled water surface to remove traces of residual metal salt solution and subsequently dried at room temperature under air overnight.

Metal Sulfide (M = Zn, Cd) Thin Film Synthesis. 0.15 mmol metal hydroxide nitrate (~20 mg; mm^2 sized fragments of thin film) were combined with 10 mL of 0.1 M sodium sulfide solution (6−8 fold molar excess) in a sealed test tube. For $Cd(OH)(NO_3) \cdot H_2O$ an immediate change in color of the solid material upon addition of the sodium sulfide solution (white to orange) indicates the formation of metal sulfide material. $Zn_5(OH)_8(NO_3)_2 \cdot 2H_2O$ and ZnS are both white in color. To ensure complete conversion to metal sulfide film, the ZnS suspension was heated to 50 °C and kept at this temperature for 4 h; CdS suspensions were kept at 90 °C for 4 h. After this time, the supernatant was removed, and the solid material washed repeatedly with doubly distilled water until the supernatant solution was no longer basic. The metal sulfide film fragments were then filtered from solution and dried at room temperature under air overnight.

Analysis and Instrumentation. All metal hydroxide nitrate and metal sulfide products were characterized to confirm their chemical composition, structural properties, and morphologies. Powder X-ray diffraction (XRD) studies used a Philips XPERT Powder Diffractometer with monochromatic Cu Kα radiation (λ = 1.540 Å), Bragg−Brentano geometry. Brunauer−Emmett−Teller (BET) surface area was determined through nitrogen adsorption isotherms at −169 °C with a TriStar 3000 instrument. Prior to analysis, larger fragments of thin film material were crushed to fit into the measurement tube, all samples were degassed at 50 °C for 3 h under N_2 flow. The BET model was used for data fitting. Scanning electron microscopy (SEM) was performed using a Tescan Vega 5130 SEM. Transmission electron microscopy (TEM) of ground and sonicated samples was performed using a FEI Tecnai G2 Sphera Microscope (200 kV). To confirm elemental composition, X-ray photoelectron spectroscopy (XPS) was performed using a Kratos Axis Ultra with a monochromated aluminum anode. The binding energy of C 1s in all spectra was shifted to 284.8 eV. UV/vis spectra were recorded using a Shimadzu UV 3600 UV−vis−NIR Spectrometer.

Results and Discussion

Using our previously described kinetically controlled vapor-diffusion catalysis method,[13,19,21] we prepared unsupported $Zn_5(OH)_8(NO_3)_2 \cdot 2H_2O$[13,14] and $Cd(OH)(NO_3) \cdot H_2O$[22] films from aqueous $Zn(NO_3)_2$ and $Cd(NO_3)_2$ solutions, respectively. For this synthesis method, an atmosphere saturated with ammonia is created by an equilibrium between ammonia in the dissolved state (aqueous NH_4OH solution) and in the gaseous state (in air). This gaseous catalyst, ammonia, then diffuses into the respective aqueous metal salt precursor solutions to induce a spatially and temporally developing gradient of pH. The resulting slow, kinetically and vectorially controlled hydrolysis reaction and subsequent polycondensation within the metal salt solutions yields morphologically structured films. Incorporation of the anions from the metal salt precursor leads to the formation of LDH

(23) Lieth, R. M. A. *Physics and Chemistry of Materials with Layered Structures, Vol. 1: Preparation and Crystal Growth of Materials with Layered Structures*; D. Reidel Publ. Co.: Boston, MA, 1977.

materials rather than the simple metal hydroxides usually obtained by precipitation reactions. The as-prepared films exhibit unique morphologies on the side of the thin film that had been facing the metal salt solution during the film growth. Plates or three-dimensional networks of agglomerated metal hydroxide nitrate nanoparticles form as a result of heterogeneous nucleation in this spatially directed catalytic reaction environment.[13,19] The other side of the film that was exposed to air during the film formation exhibits a continuous, smooth plane.[13,19] The areas of the as-prepared films were ~28 cm^2; however, after removing the material from the reaction medium, rinsing them in doubly distilled water, and drying, the thin films broke into smaller fragments several mm^2 in size because of handling and stress induced by the drying process. For this study, we did not attempt any optimization of these syntheses with regard to the final size of the film fragments. After rinsing excess metal salt solution off the film fragments, the metal hydroxide materials were used without further purification for post-synthesis conversion reactions to obtain the textured metal sulfide films.

Zinc Sulfide Prepared from Zinc Hydroxide Nitrate. Figure 1a shows a top-down view onto the morphologically nanostructured side of a $Zn_5(OH)_8(NO_3)_2 \cdot 2H_2O$ film prepared by vapor-diffusion catalysis. Plates, partially fused along the side edges, protruding roughly orthogonally from the continuous backplane of the material are randomly oriented in the *x*- and *y*-direction of this SEM image. Powder XRD confirms the crystallinity of the as-synthesized thin film material (see Supporting Information), and peak broadening of the 200 reflection (obtained from measuring the fwhm) suggest a crystalline correlation length of 20 nm for the material.[24] XPS data are in good agreement with the elemental composition of the structure determined by XRD (see Supporting Information).

The TEM image and electron diffraction pattern of $Zn_5(OH)_8(NO_3)_2 \cdot 2H_2O$ are shown in Figure 1b. Even after thorough grinding and sonication, mostly thin platelets of nanoparticle agglomerates up to several 100 nm in size can be detected by TEM, indicating very strong agglomeration and possibly fusion of individual nanoparticles. Smaller nanoparticles seen in the micrograph are ~24 nm in size, which is similar to the crystalline correlation length calculated from the XRD pattern using the Scherrer formula.[24] However, the 24 nm sized features observed by TEM may still represent agglomerates of nanoparticles. The inhomogeneous size distribution of the objects visible in Figure 1b supports this suggestion. For similarly prepared $Co_5(OH)_8(NO_3)_2 \cdot 2H_2O$ thin films we previously reported that the material consists of highly aligned nanoparticles.[14,25] These $Co_5(OH)_8(NO_3)_2 \cdot 2H_2O$ nanoparticles then agglomerate to form mechanically robust thin film plates, similar to the structure observed for $Zn_5(OH)_8(NO_3)_2 \cdot 2H_2O$ in this study (Figure 1a).

After heating film fragments of $Zn_5(OH)_8(NO_3)_2 \cdot 2H_2O$ in aq. Na_2S solution, the resulting ZnS exhibits an overall film morphology very similar to that of the precursor material. The SEM image depicting a top-down view onto the three-dimensional nanostructured morphology of the as-prepared ZnS film resembles that of the original $Zn_5(OH)_8(NO_3)_2 \cdot 2H_2O$ film very closely (Figure 1c). The plates protruding from the continuous backplane are visibly more porous than the starting hydroxide nitrate material. The sizes of individual fragments of thin film are still a few mm^2 in size, but overall fragments of thin film material are smaller and more brittle than for the precursor material. BET surface area measurements confirm the increased porosity of the ZnS thin films compared to the $Zn_5(OH)_8(NO_3)_2 \cdot 2H_2O$ films. The surface area increases from 24 m^2/g for $Zn_5(OH)_8(NO_3)_2 \cdot 2H_2O$ to 42 m^2/g for ZnS after conversion.

No trace of residual crystalline $Zn_5(OH)_8(NO_3)_2 \cdot 2H_2O$ can be detected in the X-ray diffractogram of ZnS thin films (see Supporting Information). The pattern observed for the as-synthesized fragments of ZnS thin film can be indexed to cubic ZnS.[26] The crystal lattice therefore not only undergoes anion exchange during the conversion reaction, but also changes from a *base-centered monoclinic* crystal system (*C*2/*m*) to a *face-centered cubic* one ($F\bar{4}3m$). Scherrer broadening[24] of the 111 and 200 reflections indicate the crystalline correlation lengths of 19 and 21 nm, respectively. This suggests that the crystallites, despite the drastic rearrangement of atoms, do not experience significant strain in any particular direction along different crystallographic orientations. Even more remarkable though is the degree of crystallinity observed for the ZnS film.

In contrast to the TEM image obtained for the ground $Zn_5(OH)_8(NO_3)_2 \cdot 2H_2O$ (Figure 1b), dispersed individual nanometer-sized particles can be seen in the ground ZnS (Figure 1d). The average particle size is 20 nm, which is in very good agreement with the crystalline correlation length of 19−21 nm calculated from the XRD data. The difference seen between the TEM images in Figure 1b and Figure 1d can be interpreted as a further consequence of the increased porosity and brittleness of the ZnS films. Even though the films display very similar morphologies on a micron length scale, the binding of individual nanoparticles that comprise the precursor and product films appears significantly weaker after the conversion reaction; consequently, the material breaks into its individual building blocks during the sample preparation for TEM.

XPS analysis further confirmed the complete conversion of the structured films to ZnS. In a low resolution survey scan (see Supporting Information) no peaks indicating the presence of either nitrogen or sodium could be detected. The atomic ratio of Zn to S in the low resolution scan is about 1:2. High resolution scans for Zn 2p3/2 and S 2p are shown in Figure 2a and 2b, respectively. These data indicate the presence of Zn^{2+} with the 2p3/2 peak centered at 1021.4 eV

(24) Hammond, G. S. *An introduction to crystallography and diffraction*; Oxford University Press: Oxford, 1998.
(25) Schwenzer, B.; Neilson, J. R.; Sivula, K.; Woo, C.; Fréchet, J. M. J.; Morse, D. E. *Thin Solid Films* **2008**, submitted for publication.
(26) JCPDS file No. 01-077-2100.

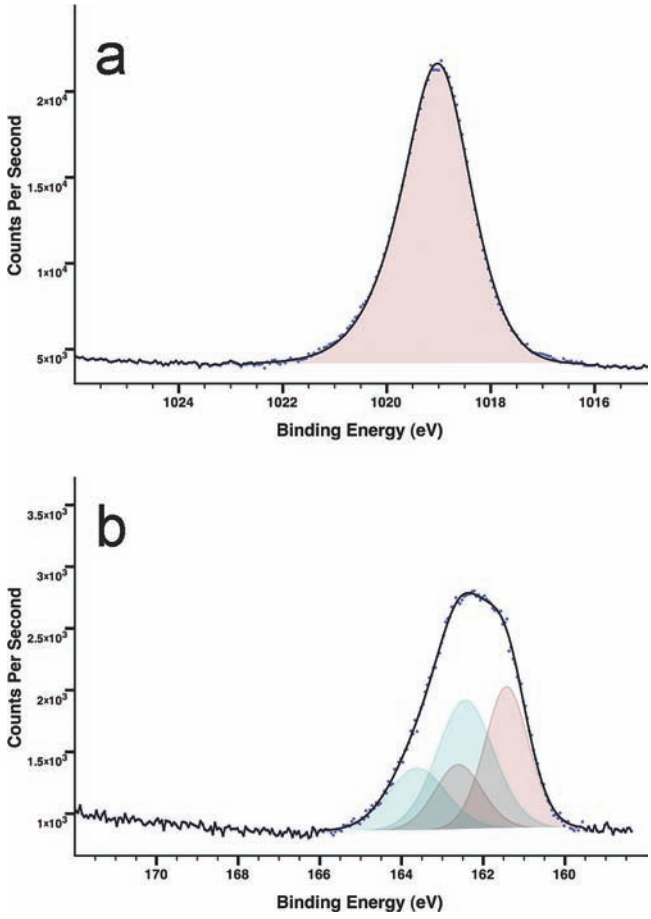

Figure 2. High resolution XPS spectra of (a) the Zn 2p3/2 region for ZnS and (b) the S 2p region for ZnS. The dotted lines indicate experimental data; the solid lines are fitted curves.

(Figure 2a). The peak position and shape are consistent with literature values reported for ZnS.[27]

The spectrum for S 2p shows a broad feature centered at 161.9 eV, which can be deconvoluted into two sets of peaks (2p1/2 and 2p3/2 each). According to literature reports, the lower energy peak at 161.4 eV originates from S^{2-} in ZnS,[27] whereas the peak at higher energy (162.4 eV) is due to elemental sulfur, S^0, or partially oxidized S^{2-} in the form of S_n^{2-}.[28] The ratio of these two peaks is ~9:11. If only the area of the peaks associated with S^{2-} in ZnS is used, the ratio of Zn to S in the thin film material is calculated to be about 1:1.2, confirming the formation of stoichiometric ZnS. For our synthesis method, the presence of elemental sulfur might be explained by the large excess of Na_2S used in the reaction. However, an enrichment of elemental sulfur on the surface of ZnS nanostructures has been observed previously;[29] we therefore conclude that this side product is not uniquely inherent to our method of film preparation.

(27) *Practical Surface Analysis by Auger and X-ray Photoelectron Spectroscopy*; Briggs, D.; Seah, M. P., Eds.; John Wiley and Sons: Chichester, U.K., 1983.

(28) (a) Hyland, M. M.; Bancroft, G. M. *Geochim. Cosmochim. Acta* **1989**, *53*, 367. (b) Toniazzo, V.; Mustin, C.; Portal, J. M.; Humbert, B.; Benoit, R.; Erre, R. *Appl. Surf. Sci.* **1999**, *143*, 229.

(29) (a) Dustan, D. E.; Hagfeld, A.; Almgren, M.; Siegbahn, H. O. G.; Mukhtar, E. *J. Phys. Chem.* **1990**, *94*, 6797. (b) Ye, C.; Fang, X.; Li, G.; Zhang, L. *Appl. Phys. Lett.* **2004**, *85*, 3035.

Cadmium Sulfide Prepared from Cadmium Hydroxide Nitrate. $Cd(OH)(NO_3)\cdot H_2O$[22] films prepared by vapor-diffusion catalysis exhibit a three-dimensional morphology on the textured side of the material different from that observed for $Zn_5(OH)_8(NO_3)_2\cdot 2H_2O$. A lacey three-dimensional network with round or oval openings can be seen in the SEM images of the top-side view of the $Cd(OH)(NO_3)\cdot H_2O$ film in Figure 3a. The frame of the network is not composed of seemingly solid material like the plates observed for $Zn_5(OH)_8(NO_3)_2\cdot 2H_2O$, but the morphology can rather be described as a construct of fused strands of material. Individual strands as thin as ~150 nm can be detected (inset in Figure 3a).

The XRD pattern can be indexed to $Cd(OH)(NO_3)\cdot H_2O$[22] (see Supporting Information). On the basis of the fwhm of the 020 reflection at 12.8° a crystalline correlation length of 28 nm is calculated for $Cd(OH)(NO_3)\cdot H_2O$ thin film material. However, this material exhibits a rapid decay in crystallinity. Within a few hours it completely loses its crystallinity, probably because of the absorption of moisture and CO_2 from the air. The calculated crystalline correlation length of the fresh material is therefore not applicable to the material after standing.

Because of the instability of $Cd(OH)(NO_3)\cdot H_2O$ the sample for TEM analysis was prepared from freshly synthesized material and kept under nitrogen until analyzed. Similar to the TEM image of $Zn_5(OH)_8(NO_3)_2\cdot 2H_2O$ in Figure 1b, very few individual nanoparticles can be observed in the micrograph of $Cd(OH)(NO_3)\cdot H_2O$ (Figure 3b). The average particle size is 32 nm, but rod-like agglomerates of nanoparticles dominate the image. These agglomerates are a few hundred nm in width and vary in length up to several μm. A selected area diffractions pattern suggests a quasi-single crystalline quality of the sample, indicating that the individual nanoparticles are highly aligned within the rod-like agglomerates. We previously observed areas of apparent single crystallinity in $Co_5(OH)_8(NO_3)_2\cdot 2H_2O$ thin films prepared by vapor-diffusion catalysis,[14] but subsequent dark field TEM revealed that this material consists of highly aligned nanoparticle arrays.[25] We therefore assume this also is the case for the rod-like structures observed in the $Cd(OH)(NO_3)\cdot H_2O$ sample.

XPS analysis was attempted to further characterize the material, but because of the chemical instability of the films, the result is inconclusive. The presence of Cd^{2+} was confirmed, but the Cd:O:N ratio could not be determined, in part because the N 1s peak is buried underneath the Cd 3d peaks.

SEM images in Figure 3c show the textured morphology of CdS films prepared from reacting $Cd(OH)(NO_3)\cdot H_2O$ with aqueous Na_2S solution. The similarity between the morphology of the CdS film and that of the starting material again indicates a good retention of morphology despite atomic rearrangements during the reaction. BET surface area measurements reveal that for this material system the surface area significantly increases from 15 m^2/g to 50 m^2/g during

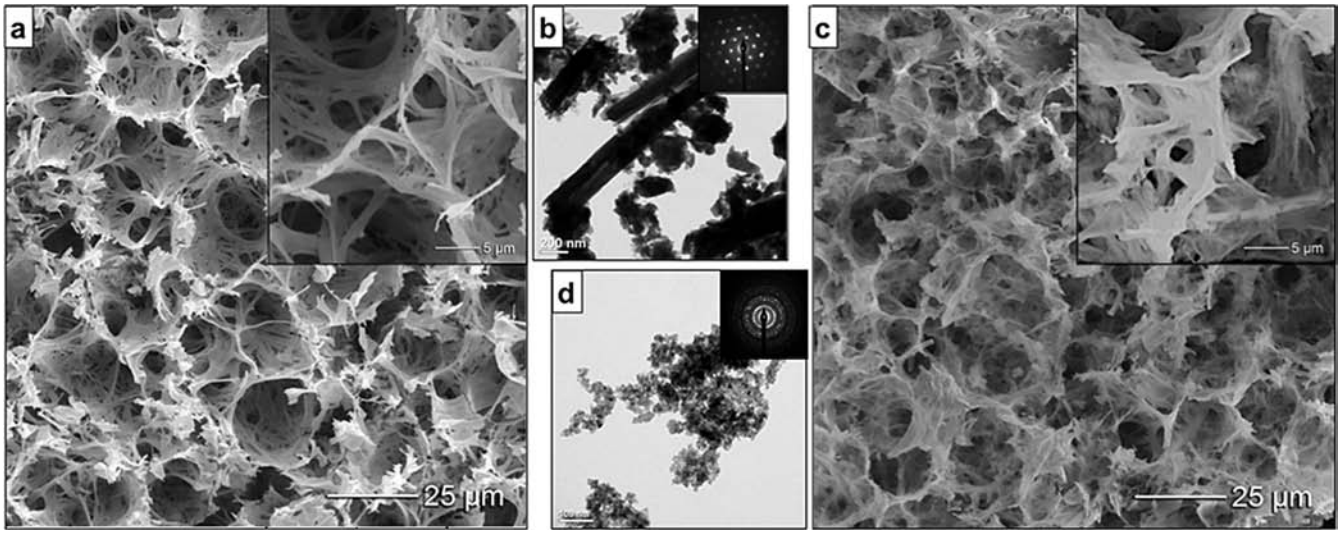

Figure 3. Nanostructured $Cd(OH)(NO_3)\cdot H_2O$ film prepared as described in the text: (a) SEM image of the nanostructured side of the film [inset: higher resolution SEM image], (b) TEM image of ground material [inset: SAED image]; CdS film synthesized using as-prepared $Cd(OH)(NO_3)\cdot H_2O$ films: (c) SEM image of the nanostructured side of the film [inset: higher resolution SEM image], (d) TEM image of the ground material [inset: SAED image].

the conversion from the metal hydroxide nitrate to the metal sulfide.

The XRD pattern recorded from the as-synthesized CdS films exhibits weak overall peak intensities (see Supporting Information), but despite the seemingly large proportion of amorphous material (most likely because of decomposition of the starting material before the conversion reaction), *cubic* CdS[30] can be identified as the main crystalline phase in the sample. This system thus undergoes a change from a *primitive orthorhombic* crystal system (*Pbca*) for $Cd(OH)(NO_3)\cdot H_2O$[22] to a *face-centered cubic* system ($F\bar{4}3m$) for CdS during the reaction. Traces of *hexagonal* CdS[31] also can be identified in the XRD spectrum (peaks at 29°, 36°, 48°). Peak broadening of the 111 reflection for the *cubic* phase at 26.5° (obtained from measuring the fwhm) suggests a crystalline correlation length of 21 nm for the dominant polymorph.[24]

In contrast to the TEM image obtained for $Cd(OH)(NO_3)\cdot H_2O$ (Figure 3b), dispersed individual nanometer-sized particles of CdS can be seen in Figure 3d. The average particle size is 19 nm, which is in good agreement with the crystalline correlation length of 21 nm calculated from the XRD data. Selected area electron diffraction confirms the sample's principal composition as *cubic* CdS.[30]

XPS analysis indicates the complete conversion of the material to CdS. In a low resolution survey scan (see Supporting Information), no peaks indicating the presence of sodium could be detected either. The percentage of oxygen observed is the same as for the data obtained for ZnS and therefore attributed to either surface bound oxygen on the CdS film or oxygen contamination from the carbon adhesive tape beneath the sample. The high resolution spectrum in Figure 4a indicates the presence of Cd^{2+} with the 3d5/2 peak centered at 404.7 eV and the 3d3/2 peak at 411.5 eV. The peak position and shape are consistent with literature values reported for CdS.[32] The atomic ratio of Cd to S in the low resolution scan is 1:1. In contrast to the spectra for ZnS, only one species of sulfur can be detected in the range indicative of CdS.[32] The S 2p1/2 and S 2p3/2 peaks are centered at 161.1 and 162.3 eV, respectively (Figure 4b). The broad peak of weak intensity at 167.7 eV suggests the presence of SO_4^{2-}, a possible photocorrosion product that previously has been observed as a decomposition product

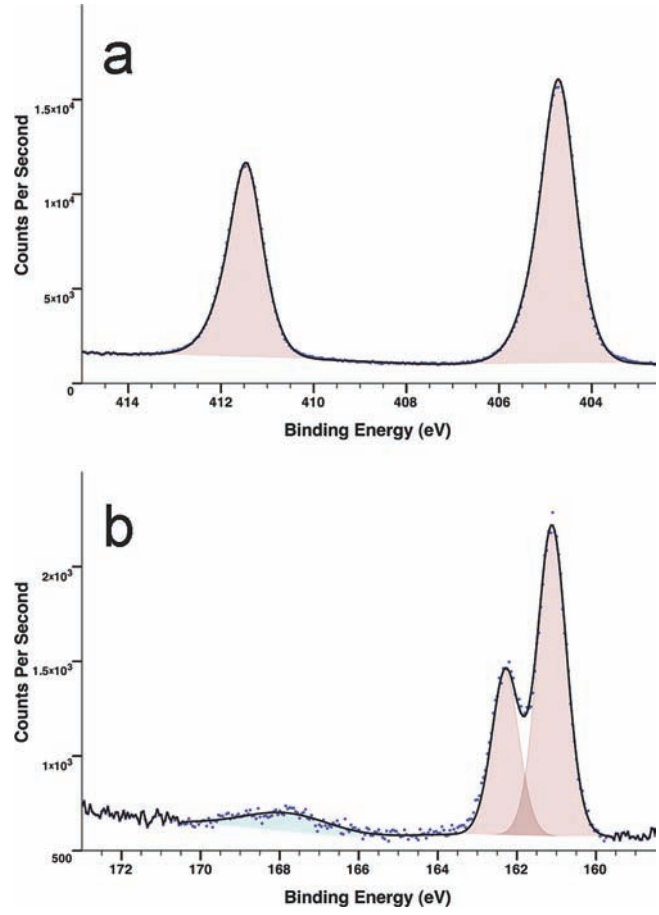

Figure 4. High resolution XPS spectra of (a) the Cd 3d region for CdS and (b) the S 2p region for CdS. The dotted lines indicate experimental data; the solid lines are fitted curves.

(30) JCPDS file No. 01-080-0019.
(31) JCPDS file No. 01-080-006.

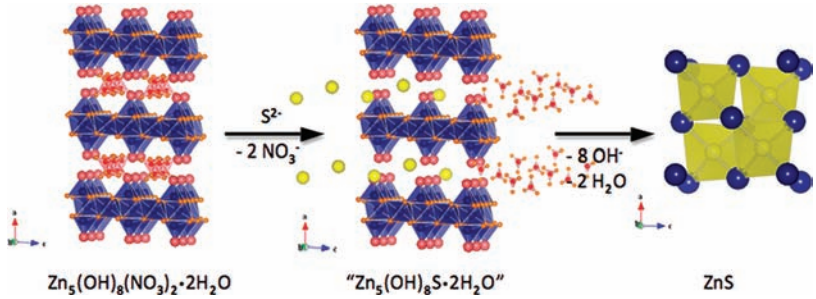

Figure 5. Schematic of the proposed anion exchange/solid state conversion reaction sequence for the conversion of $Zn_5(OH)_8(NO_3)_2 \cdot 2H_2O$ to ZnS.

of other metal sulfides.[29] Elemental sulfur could not be detected in the S 2p region of the XPS spectrum. However, the S 2p3/2 peaks of elemental sulfur and CdS are only separated by 0.1 eV and a non-distinguishable percentage of S^0 might be present in this sample as well.

General Discussion. The conversion reactions described for the Zn- and Cd-based systems occur quickly upon addition of the aqueous Na_2S solution. For $Cd(OH)(NO_3) \cdot H_2O$ an immediate change in color of the solid material upon addition of the sodium sulfide solution (white to orange) indicates the formation of the metal sulfide. (As noted above, $Zn_5(OH)_8(NO_3)_2 \cdot 2H_2O$ and ZnS are both white in color.) In contrast to the conventional CBD,[20] the method we report here relies on the conversion of an already existing solid state material in nanostructured film morphology, rather than on the formation of a metal sulfide film from metal complexes in solution. Possibly because of the open crystal structure of the LDH precursor materials, diffusion of the sulfide anions into the existing solid state structure does not seem to be a factor limiting the overall conversion yield—at least under the conditions reported here. A reaction time of 4 h, as employed for this study, yields complete conversion to metal sulfides with no detectable traces of residual metal hydroxide nitrate, while not allowing significant erosion of the three-dimensional structure of the metal sulfide. Shorter reaction times lead to incomplete conversion while longer reaction times result in a decrease in film thickness of the material, indicating chemical etching caused by the strongly basic reaction conditions. The conversion reactions of metal hydroxide nitrate films to metal sulfide materials commence at an initial pH of ~12.4, decreasing slightly to pH ~12.2 during the course of the reaction. At this high pH, the predominant hydrogen sulfide species in solution is the fully deprotonated S^{2-}.[33]

The equations describing the stoichiometric conversion from the LDH materials to the respective metal sulfides are as follows:

$$Zn_5(OH)_8(NO_3)_2 \cdot 2H_2O + 5S^{2-} \rightarrow 5ZnS + 8OH^- + 2NO_3^- + 2H_2O \quad (1)$$

$$Cd(OH)(NO_3) \cdot H_2O + S^{2-} \rightarrow CdS + OH^- + NO_3^- + H_2O \quad (2)$$

On the basis of these reactions, the slight decrease in pH over the course of the reaction might be attributed to the release of NO_3^- anions, a weak base, and the simultaneous depletion of S^{2-}, a relatively strong base, from the aqueous reaction solution.

Comparison of the enthalpy values (heat of formation; ΔH_f) for $Zn(OH)_2$ versus ZnS and $Cd(OH)_2$ versus CdS suggests that reactions 1 and 2 might be thermodynamically unfavorable.[34] Although several reports describe solid state conversion reactions yielding ZnS nanostructures from ZnO nanostructures,[3] we believe it is unlikely that the LDH films decompose to their respective metal oxides under these conditions and then react to form metal sulfide films while retaining the observed remarkable degree of connectivity throughout two crystallographic rearrangements. We have not been able to detect any evidence suggesting such a reaction pathway.

Since this solid state conversion reaction is carried out in water, we assumed that an excess of S^{2-} anions would be needed to drive the reaction to completion. Experiments varying the stoichiometric molar ratio of metal hydroxide nitrate and Na_2S support this suggestion. The conversion reactions under conditions of equal stoichiometry were incomplete, leaving residual starting material or traces of the respective metal oxide detectable by XRD.

Furthermore, the presence of elemental sulfur on the surface of the ZnS films, as observed by XPS, suggests that at least for this reaction, a certain percentage of the hydrogen sulfide species present in the reaction solution becomes oxidized and bound. This might explain why a slight excess of Na_2S (6−8 fold) is needed to yield complete conversion. However, when a large excess of S^{2-} anions is supplied, such as a 50-fold excess, a decrease in crystallinity of the final metal sulfide material is observed, and the retention of the three-dimensional morphology of the thin films diminishes noticeably as well. Our experiments thus suggest that the favorable increase in entropy during the reactions 1 and 2 plays a significant role in the overall thermodynamic equation, helping to drive the reaction to completion despite the large excess of available OH^- ions in solution.

The layered crystal structure and high porosity of the LDH films further aid in the anion exchange reaction that is concomitant with significant rearrangements of the lattice structure. Figure 5 illustrates the proposed anion exchange/solid state conversion reaction sequence.

(32) Barreca, D.; Gasparotto, A.; Maragno, C.; Tondello, E. *Surf. Sci. Spectra* **2002**, *9*, 46.
(33) Haimour, N.; El-Bishtawi, R.; Ail-Wahbi, A. *Desalination* **2005**, *181*, 145.
(34) *Handbook of Chemistry and Physics*, 57th ed.; CRC Press, Inc.: Cleveland, OH, 1976.

The remarkable retention of the three-dimensional nanostructured morphology for the metal sulfide thin films compared to the metal hydroxide nitrate starting material is especially surprising when the rearrangements of lattice parameters during the conversion reaction are considered. For both solid state conversion reactions the resulting product, the metal sulfide, exhibits higher crystal symmetry than the rather complex structures of the starting materials, $Zn_5(OH)_8(NO_3)_2 \cdot 2H_2O$ or $Cd(OH)(NO_3) \cdot H_2O$.

The $Zn_5(OH)_8(NO_3)_2 \cdot 2H_2O$/ZnS system undergoes a change from a *base-centered monoclinic* Bravais lattice to a *face-centered cubic* one, involving compression of the lattice parameters, particularly along the *a*-axis ($a = 19.4800$ Å for $Zn_5(OH)_8(NO_3)_2 \cdot 2H_2O$[14] and $a = 5.4145$ Å for ZnS[26]). The volume of the unit cell decreases from $Zn_5(OH)_8(NO_3)_2 \cdot 2H_2O$ to ZnS and the packing density of the Zn^{2+} ions in the crystal structure increases as the coordination environment for the Zn^{2+} ions changes from mostly octahedral in $Zn_5(OH)_8(NO_3)_2 \cdot 2H_2O$ to purely tetrahedral in ZnS. The hydrotalcite-like structure of $Zn_5(OH)_8(NO_3)_2 \cdot 2H_2O$ exhibits a ratio of 3:2 octahedral to tetrahedral sites in the charged cationic layers that are held together by intercalated NO_3^- anions and water molecules.[13] Although the main coordination number for Zn^{2+} in $Zn_5(OH)_8(NO_3)_2 \cdot 2H_2O$ is 6 within the cationic sheets, an overall lower crystal density results from the layered crystal structure. In *cubic* ZnS the coordination number is reduced to 4. Zn^{2+} ions can only accommodate four S^{2-} anions in the first coordination sphere, and therefore are tetrahedrally coordinated, because of the larger ionic radius of S^{2-} (170 pm)[35] compared to OH^- (123 pm)[35] in the packed cationic layers of $Zn_5(OH)_8(NO_3)_2 \cdot 2H_2O$.

During the $Cd(OH)(NO_3) \cdot H_2O$ to CdS conversion the crystal system similarly rearranges from *primitive orthorhombic* to *face-centered cubic*. The unit cell of CdS ($a = b = c = 5.8110$ Å[30]) is compressed in all directions compared to $Cd(OH)(NO_3) \cdot H_2O$ ($a = 8.7420$ Å, $b = 13.9300$ Å, $c = 6.9330$ Å[22]). A decrease in specific volume and an increase in packing density for the Cd^{2+} ions results as discussed for ZnS above.

Zinc sulfide (band gap of 3.54 eV) and cadmium sulfide (band gap of 2.42 eV) were chosen as target products to demonstrate this novel synthesis approach because these are two widely used II−VI semiconducting materials. Among other applications, both metal sulfides and several of their alloys with other metals or chalcogens are used as phosphors,[36] in photovoltaic devices,[37] as biosensors[38] and for photocatalytic reactions.[39,40] For example, their role in the photocatalytic generation of hydrogen gas recently has received increased attention.[40]

UV/vis measurements of the ZnS and CdS thin films reveal that despite their nanostructured morphologies their optical properties are the same as have been reported for the bulk materials.[41] With crystalline correlation lengths well above 10 nm, no effects of quantum confinement in the optical properties could be detected (see Supporting Information). ZnS exhibits a band edge of 353 nm (3.51 eV), which is in good agreement with the value for bulk *cubic* ZnS (3.54 eV).[41] For CdS a band gap of 514 nm (2.41 eV) was measured, matching the reported band edge for bulk CdS of 2.42 eV.[41] This indicates that the CdS films are of good quality with regard to their desired optical properties despite the presence of traces of amorphous material and *hexagonal* CdS.

In both cases the surface area of the metal sulfide thin films is significantly larger than for the LDH material. The calculated crystalline correlation length, as well as the average size of individual nanoparticles determined from TEM images decrease from the $Zn_5(OH)_8(NO_3)_2 \cdot 2H_2O$ starting material (~30 nm) to ZnS (~20 nm). The same trends, although not as pronounced, are observed for the conversion of $Cd(OH)(NO_3) \cdot H_2O$ to CdS. This decrease in particle size, either accompanied by or resulting from a decrease in specific volume of the crystallites, leads to the observed material shrinkage upon anion exchange. Considering the overall retention in morphology for the films coupled with this nanoparticle contraction, the observed increase in surface area for the metal sulfide materials is no surprise. BET measurements reveal that the LDH materials, as well as the metal sulfide films, have relatively large mesopores (~50 nm), and the shape of the adsorption isotherms shows no indication that smaller nanopores (<5 nm) are present (see Supporting Information). This suggests that the total surface area of these materials should easily be accessible for catalytic purposes. With 42 m^2/g and 50 m^2/g for ZnS and CdS, respectively, the materials display surface area values that are in the range of what is currently used for some catalytic conversion applications. The overall surface area of the material can be further enhanced by depositing the films onto macroporous substrates, a technique that is frequently used in catalyst design.[39,40]

Conclusion

In summary, we have demonstrated the first solid state conversion reaction to form micrometer-sized three-dimensionally structured ZnS and CdS films at low temperatures. On the basis of an anion exchange reaction in LDH films, $Zn_5(OH)_8(NO_3)_2 \cdot 2H_2O$ and $Cd(OH)(NO_3) \cdot H_2O$, this method offers a novel approach to use LDH materials simultaneously as precursors and templates in solid state conversion reactions to synthesize nanostructured metal sulfide films. We have

(35) Shannon, R. D. *Acta Crystallogr.* **1976**, *A32*, 751.
(36) (a) Wilcoxon, J. P.; Newcomer, P. *Proc. SPIE-Int. Soc. Opt. Eng.* **2002**, *4808*, 99. (b) Qi, L.; Lee, B. I.; Morton, D.; Forsythe, E. *Mater. Eng.* **2005**, *28*, 217.
(37) (a) Morales-Acevedo, A. *Solar Energy* **2006**, *80*, 675. (b) Goudarzi, A.; Aval, G. M.; Sahraei, R.; Ahmadpoor, H. *Thin Solid Films* **2008**, *516*, 4953. (c) Shen, Q.; Kobayashi, J.; Diguna, L. J.; Toyoda, T. *J. Appl. Phys.* **2008**, *103*, 084304. (d) Thanachayanont, C.; Inpor, K.; Sahasithiwat, S. *J. Korean Phys. Soc.* **2008**, *52*, 1540.
(38) (a) Jie, G.; Liu, B.; Pan, H.; Zhu, J.-J.; Chen, H.-Y. *Anal. Chem.* **2007**, *79*, 5574. (b) Li, H.; Shih, W. Y.; Shih, W.-H. *Nanotechnology* **2007**, *18*, 205604.
(39) (a) Stroyuk, A. L.; Sobran, I. V.; Korzhak, A. V.; Raevskaya, A. E.; Kuchmiy, S. Y. *Colloid Polym. Sci.* **2008**, *286*, 489. (b) Jang, J. S.; Y. C.-J.; Choi, S. H.; Ji, S. M.; Kim, E. S.; Lee, J. S. *J. Catal.* **2008**, *254*, 144.
(40) (a) Xing, C.; Zhang, Y.; Yan, W.; Guo, L. *Int. J. Hydrogen Engergy* **2006**, *31*, 2018. (b) Priya, R.; Kanmani, S. *Curr. Sci.* **2008**, *94*, 102. (c) Bao, N.; Shen, L.; Takata, T.; Domen, K. *Chem. Mater.* **2008**, *20*, 110.
(41) Kittel, C. *Introduction to Solid State Physics*, 7th ed.; John Wiley and Sons, Inc.: New York, NY, 1995.

shown the products exhibit a surprisingly high degree of morphological retention and crystallinity similar to the LDH precursor films. The three-dimensionally structured metal sulfide films are composed of interconnected nanoparticles (~20 nm in diameter) resulting in high surface areas. Surface areas of 42 m^2/g for zinc sulfide and 50 m^2/g for cadmium sulfide thin films are observed. These values correspond to an increase in surface area of 75% for the $Zn_5(OH)_8(NO_3)_2 \cdot 2H_2O$ to zinc sulfide conversion, while the cadmium sulfide films exhibit more than three times the surface area of their precursor material, $Cd(OH)(NO_3) \cdot H_2O$. Despite their nanoparticulate nature the ZnS and CdS films display the same optical properties as the corresponding bulk materials. The three-dimensional morphology of the resulting films is thus observed to combine the physical properties of the bulk materials with the advantages of higher surface areas typically associated with nanostructured or porous materials.

Furthermore, this study shows that the environmentally benign vapor-diffusion catalysis method can be used not only to prepare nanostructured LDH, metal oxide, or phosphate thin films,[14,19,21] but that the as-prepared LDH materials can readily be converted to metal chalcogenide thin films with similarly unique three-dimensional nanostructured morphologies. This creates new possibilities for the preparation of metal chalcogenide thin films with higher surface areas at lower cost than heretofore possible. Taking advantage of the three-dimensionally nanostructured films of these materials prepared in this manner might thus increase the efficiencies of biosensors,[38] photovoltaic devices,[37] and other applications currently using the unstructured metal sulfide films.

Acknowledgment. This work was supported by grants from the U.S. Dept. of Energy (DEFG03-02ER46006); the U.S. Army Research Office through grant DAAD19-03-D-0004 to the Institute for Collaborative Biotechnologies; and the MRSEC Program (award No. DMR05-20415) of the National Science Foundation (UCSB Materials Research Laboratory). J. R. Neilson is supported by a National Science Foundation Graduate Research Fellowship. We thank Drs. T. Mates, J. Li, and E. H. L. Falcao for their helpful suggestions.

Supporting Information Available: Powder XRD pattern of all materials. XPS data for the as-prepared $Zn_5(OH)_8(NO_3)_2 \cdot 2H_2O$ including a survey scan and high resolution spectra. XPS survey scans for ZnS and CdS thin film materials. UV/vis spectra for ZnS and CdS thin film materials. Figures of the BET adsorption and desorption isotherms for $Zn_5(OH)_8(NO_3)_2 \cdot 2H_2O$, $Cd_3(OH)_5(NO_3) \cdot H_2O$, ZnS, and CdS. This material is available free of charge via the Internet at http://pubs.acs.org.

IC801865W